Monte Carlo study of growth in the two-dimensional spin-exchange kinetic Ising model

Jacques G. Amar
Thermophysics Division, National Bureau of Standards, Gaithersburg, Maryland 20899

Francis E. Sullivan
Center for Applied Mathematics, National Bureau of Standards, Gaithersburg, Maryland 20899

Raymond D. Mountain
Thermophysics Division, National Bureau of Standards, Gaithersburg, Maryland 20899

(Received 7 May 1987)

Results obtained from extensive Monte Carlo simulations of domain growth in the two-dimensional spin-exchange kinetic Ising model with equal numbers of up and down spins are presented. Using different measures of domain size—including the pair-correlation function, the energy, and circularly-averaged structure factor—the domain size is determined (at $T=0.5T_c$) as a function of time for times up to 10^6 Monte Carlo steps. The growth law $R(t)=A+Bt^{1/3}$ is found to provide an excellent fit (within 0.3%) to the data, thus indicating that at long times the classical value of $\frac{1}{3}$ for the exponent is correct. It is pointed out that this growth law is equivalent to an effective exponent for *all* times (as given by Huse) $n_{\rm eff}(t)=\frac{1}{3}-\frac{1}{3}C/R(t)$. No evidence for logarithmic behavior is seen. The self-averaging properties of the various measures of domain size and the variation of the constants A and B with temperature are also discussed. In addition, the scaling of the structure factor and anisotropy effects due to the lattice are examined.

I. INTRODUCTION

The kinetics of domain growth in the late stages of diffusion-limited spinodal decomposition has been studied by a variety of methods. However, disagreement has remained as to the asymptotic time dependence of the average linear domain size $R(t)$ for long times t except in the limit of small concentration. Thus, for example, the classic work of Lifshitz and Slyozov[1] predicts a long-time growth law of the form $R(t)\sim t^n$ where $n=\frac{1}{3}$, in the limit of a dilute amount of one phase. On the other hand, more recent work by Mazenko *et al.*[2] on spinodal decomposition of the two-dimensional Ising model at 50% concentration, has led to the prediction of a logarithmic growth law at long times in this case. At the same time, Monte Carlo simulations of spinodal decomposition in the two- and three-dimensional Ising model (also at zero total magnetization) have found effective exponents in the range 0.17–0.25 when fitting the domain size to the power-law form.[2–5]

Recently, the Lifshitz-Slyozov theory has been generalized qualitatively to apply to the case of equal fractions of the two phases by Huse.[6] Huse's theory assumes that the rate of growth of the average domain size can be written at late times, as

$$\frac{dR}{dt}=C_2/R^2(t)+C_3/R^3(t)+O(R^{-4}) , \tag{1}$$

where C_2 corresponds to the contribution to growth from diffusion between domains through the bulk and C_3 corresponds to the first-order correction, due to the transport of spins along the interface between domains. Solving Eq. (1) for large R and t, Huse obtained the growth law

$$R(t)=A+Bt^{1/3} , \tag{2}$$

where $A=C_3/2C_2$ and $B=(3C_2)^{1/3}$. This resulted in a prediction for the effective exponent $n_{\rm eff}(t)$ at long times given by

$$n_{\rm eff}(t)=\tfrac{1}{3}-C/R(t) , \tag{3}$$

where $n_{\rm eff}(t)$ is defined by

$$n_{\rm eff}(t)=d\{\ln[R(t)]\}/d(\ln t) \tag{4}$$

and $C=\frac{1}{3}A$. Huse also presented Monte Carlo data for a 192×192 lattice consisting of an average of 21 runs up to 4000 Monte Carlo steps (MCS) and 7 runs from 4000 MCS to 40 000 MCS, at a temperature of $T=0.9T_c$, and one run (of 4000 MCS) at $T=0.5T_c$. The effective exponent in Huse's data was found to increase with time t—in agreement with his prediction. However, the uncertainty in the data led to an extrapolated long-time exponent of $n(t=\infty)=0.29\pm 0.04$—rather disappointingly far from $\frac{1}{3}$. In addition, there were large fluctuations in the later-time data.

Recently, in a detailed analysis of fluctuations in Monte Carlo simulations, it has been pointed out[7] that certain measures of domain size (such as the value of the peak of the structure function) may be quantities which are not self-averaging—i.e., whose relative error does not increase with increasing system size. In addition, it

has been emphasized that even for quantities which are self-averaging, one still needs to do averages over a large number of runs (possibly up to 1000) in order to get good results for growth exponents. At the same time, other measures of domain size, such as the first moment of the structure factor, were not studied in Ref. 6. Thus, it was felt that a more extensive study, involving a larger number of runs and a longer simulation time, as well as a variety of measures of domain size, would be useful. In addition, the choice of a fairly large (512×512) system would decrease the errors due to finite-size effects and increase the statistics for those quantities measured which are indeed self-averaging.

In this paper, we discuss the results of such a more extensive study, using a novel multispin Monte Carlo algorithm. Our results suggest strongly that the classical value of $\frac{1}{3}$ (e.g., 0.330 ± 0.005) is indeed the correct exponent in the asymptotic time regime, with the effective exponent varying linearly with $1/R$ for intermediate and late times, in agreement with the qualitative behavior predicted by Huse. More strikingly, perhaps, we find that a growth law of the form $R(t)=A+Bt^{1/3}$ provides an excellent fit to our data. At the same time we see clearly the effects of the lattice in our simulations. We also discuss scaling, including slight deviations therefrom, and the dependence of the coefficients A and B from our fit as a function of temperature and coverage. In particular, while the observed variation of the long-time coefficient B with temperature (at low temperature) agrees quite well with the predictions of Huse, the coefficient A appears to increase more slowly with decreasing temperature than indicated by the arguments of Ref. 6. The self-averaging properties of our various measures of domain size are also discussed.

II. MONTE CARLO SIMULATIONS

Our Monte Carlo simulations were conducted, using the standard Metropolis algorithm,[8] on a 512×512 square lattice with isotropic nearest-neighbor couplings J and periodic boundary conditions. Using the binary representation of an Ising spin as 1 bit of a 64-bit word, we were able to store the entire lattice as one 4096-word binary array. However, instead of simply attempting one spin exchange at a time, we used an efficient vectorizable algorithm[9] involving a form of multispin coding which is an extension of the "checkerboard" algorithm[10] used in multispin simulations of the Ising model with spin-flip dynamics. In our scheme, the 512×512 lattice is broken up into a 128×128 array of 4×4 sublattices (see Fig. 1). Equivalently, each set of corresponding spins in each sublattice can be thought of as one of 16 planes or vectors. One "vectorized exchange" then corresponds to allowing all the spins from one plane to attempt to exchange with all the spins from another nearest-neighbor plane. This algorithm was particularly efficient because exchanges could then be implemented using hardware logical vector operations on the Cyber 205. (The use of "if statements," which prevent vectorization, was avoided by using the technique of "demon bits" in a manner similar to that used by Bhanot *et al.*[11]

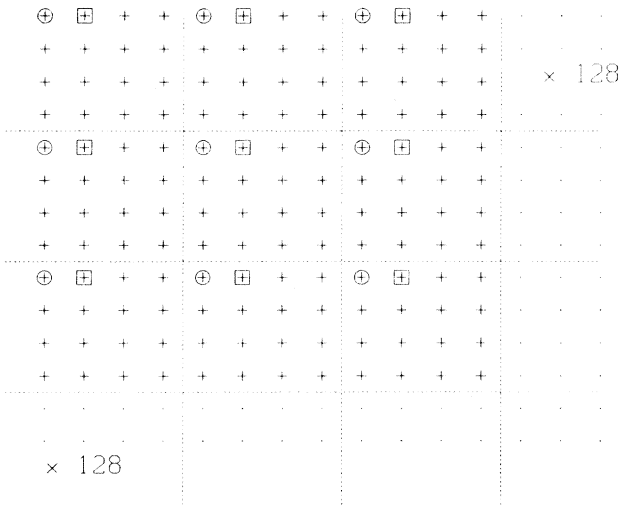

FIG. 1. Schematic showing decomposition of 512×512 lattice into 16 (128×128) sublattices (pluses correspond to lattice sites). The circled sites correspond to one (128×128) sublattice or "vector" while the sites labeled by a square correspond to another. Each "vectorized exchange" corresponds to attempted exchange of 1 pair of (128×128) nearest-neighbor sublattices. One MCS corresponds to 32 "vectorized exchanges."

for equilibrium simulations of the three-dimensional Ising model.) The choice of which pair of planes or vectors to try to exchange is made randomly and (since there are 32 pairs of possible types of exchanges) each 32 sets of "attempted vectorized exchanges" corresponds to one Monte Carlo step. This resulted in a fairly efficient code in which we achieved a simulation rate of about 15×10^6 attempted exchanges per second[12] or equivalently about 28.5 MCS per second. We note that, because the pair to be exchanged is chosen randomly, we did not expect there to be any problem with "marching" or false correlations. A similar type of multispin coding has already been used and found to compare favorably with ordinary Monte Carlo in a study of domain growth in the Ising model with spin-flip dynamics by Gawlinski *et al.*[13]

Our lattice of spins was prepared in a random (infinite-temperature) state, after which spins were randomly flipped until a state consisting of an equal number of up and down spins was achieved. A run then consisted of quenching the system to a temperature below T_c and conducting the simulation. Our data consist of 100 runs of 100 000 MCS at $T=0.5T_c$ and 10 runs of 10^6 MCA at $T=0.5T_c$. (A temperature of $0.5T_c$ was selected partly because this is low enough so that thermal fluctuations would not be too large and also because previous work has already been done[6] at this temperature with which we could compare our data.) In addition, we have conducted one additional run of 10^6 MCS at $T=0.3T_c$. Figure 2 shows the configuration of the lattice at three different times in the course of a run.

Data taken included the two-dimensional structure factor

$$S(\mathbf{k},t)=\left\langle \left| (1/N)\sum_{\mathbf{r}_i} s(\mathbf{r}_i,t)\exp(i\mathbf{k}\cdot\mathbf{r}_i) \right|^2 \right\rangle \tag{5}$$

with $\mathbf{k}=(2\pi/L)(m\mathbf{i}+n\mathbf{j})$ and $m,n=1,2,3,\ldots,L$ [where $N=(512)^2$ is the number of spins, and $L=512$ is the dimension of the system, and the angular brackets denote an average over the number of runs], the two-dimensional pair-correlation function $g(\mathbf{r};t)=\langle s(\mathbf{0},t)s(\mathbf{r},t)\rangle$ (also averaged over the number of runs), and in addition the average of the squares of both the structure factor and pair-correlation function. In addition to the structure factor, a further average was taken to smooth the results—the circularly-averaged structure factor, defined as

$$\hat{S}(k_n,t)=\sum_{\mathbf{k}}{}' S(\mathbf{k},t)\Big/\sum{}' 1, \quad k_n=2\pi n/L \tag{6}$$

where $n=0,1,2,\ldots,256$ and each sum $\sum'$ for a given value of n is over a spherical shell defined by

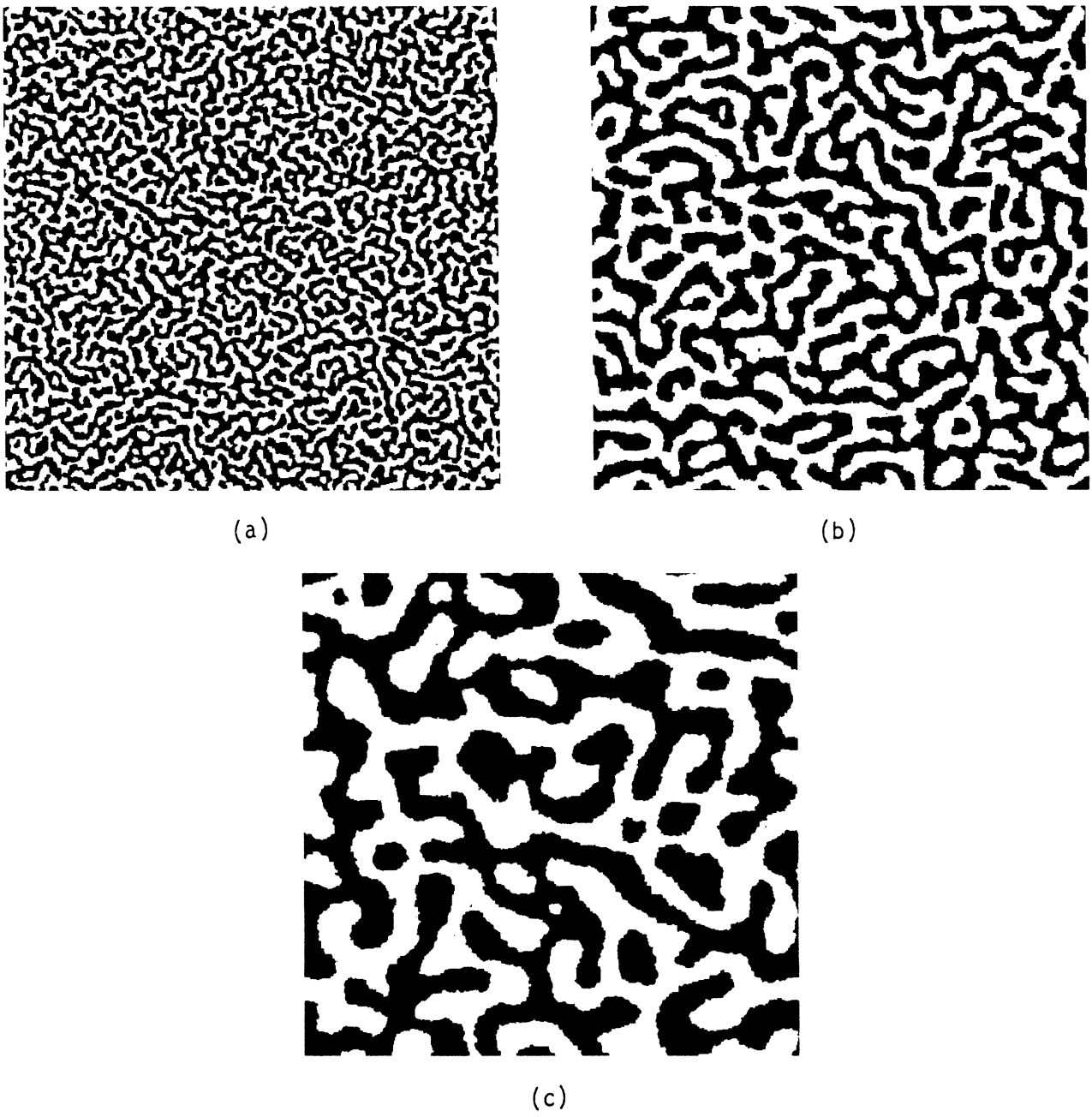

FIG. 2. View of 512×512 lattice in the course of one run (at $T=0.5T_c$) at three different times: (a) 5000 MCS, (b) 100 000 MCS, and (c) 980 000 MCS.

$$n-\tfrac{1}{2}\leq(L/2\pi)\,|\,\mathbf{k}\,|<n+\tfrac{1}{2}\ . \tag{7}$$

For the 100 runs of 100 000 MCS, configurations were saved and data were taken at intervals of 2000 MCS up to 40 000 MCS, and at intervals of 5000 MCS thereafter, resulting in 32 data points per run. For the 10^6-MCS runs, data were taken every 5000 MCS, resulting in 200 data points over the course of a run.

The domain size $R(t)$ was monitored using the following three methods.

(1) From the energy per spin $E(t)$,

$$R_E(t)=2J/[E(t)-E_0]\ , \tag{8}$$

where E_0 is the equilibrium energy per spin at temperature T from the Onsager solution.[14] This "inverse perimeter density" has been suggested as a measure of domain size in a previous study by Sadiq and Binder[15] and has been used in a number of previous studies of domain growth.[13,15]

(2) From the pair-correlation function $g(\mathbf{r};t)$, we proceed as follows. The average of the pair-correlation function along the x and y axes ($g_{xy}(r,t)=\frac{1}{2}[g(r,0;t)+g(0,r;t)]$) and along the two-body diagonals ($g_{dd}(\sqrt{2}r,t)=\frac{1}{2}[g(r,r;t)+g(-r,r;t)]$) was obtained and from each an estimate of domain size [$RG_{xy}(t)$ and $RG_{dd}(t)$, respectively] was taken as the point at which the functions $g_{xy}(r,t)$ and $g_{dd}(r,t)$, respectively, crossed zero. [The three points in $g_{xy}(r,t)$ and $g_{dd}(r,t)$ closest to zero were fit to a quadratic function and $R(t)$ defined as the value of r for which this function vanishes, as in Ref. 6.] The domain size $R_G(t)$ was then taken as the average of $RG_{xy}(t)$ and $RG_{dd}(t)$.

(3) From the first and second moments of the circularly-averaged structure factor $\hat{S}(k,t)$,

$$R_1(t)=2\pi/k_1(t)$$

with (9)

$$k_1(t)=\sum_{k_n=0}^{k_c}k_n\hat{S}(k_n,t)\Big/\sum_{k_n=0}^{k_c}\hat{S}(k_n,t)\ ,$$

$$R_2(t)=2\pi/\sqrt{k_2(t)}$$

with (10)

$$k_2(t)=\sum_{k_n=0}^{k_c}k_n^2\hat{S}(k_n,t)\Big/\sum_{k_n=0}^{k_c}\hat{S}(k_n,t)\ ,$$

where $k_n=2\pi n/L$, $n=0,1,2,3,\ldots,n_c$ and $k_c=2\pi n_c/L$. We note that the numerators of both expressions depend somewhat sensitively on the value used for the cutoff k_c. However, we note that the sum rule

$$\sum_{\text{all }\mathbf{k}}\sum S(\mathbf{k},t)=1$$

implies the approximate sum rule (exact in the limit of isotropic structure factor and large L),

$$\sum k\hat{S}(k,t)=1/2\pi\ . \tag{11}$$

[In the limit that the lattice size L becomes very large this becomes an integral; see Eq. (17).] Thus, to minimize as far as possible the statistical error in the evaluation of R_1 we substituted in the numerator of the first expression the sum-rule value $\frac{1}{2}\pi$ and used for the cutoff n_c the maximum possible value ($n_c=256$ or half the lattice size). [The calculated value of $\sum_{k_n=0}^{k_c}k_n\hat{S}(k_n,t)$ from our simulation using a cutoff value of $n_c=256$ varied by less than 1% from this value.]

Using the three methods just mentioned, the average domain size $R(t)$ as a function of time (averaged over the number of runs) was obtained. In addition, the variance $\Delta R(t)$—calculated from the fluctuations from run to run—was also obtained as

$$\Delta R(t)=[\langle R^2(t)\rangle-\langle R(t)\rangle^2]^{1/2}\ . \tag{12}$$

From the variance $\Delta R(t)$, the estimated statistical error $\delta R(t)$ was calculated as

$$\delta R(t)=\Delta R(t)/(N_r-1)^{1/2}\ , \tag{13}$$

where N_r (equal to 10 or 100) is the number of runs.

III. RESULTS

A. Pair-correlation function and energy data

1. Domain size

Figures 3 and 4 show log-log plots of $R_G(t)$ and $R_E(t)$ as a function of the number of MCS for our 10^5- and 10^6-MCS runs. We note that the increasing slope indicates that the effective exponent is increasing with time and thus the growth exponent has yet to reach its asymptotic value. We also note that the two curves in each figure appear to be "parallel" and thus in agreement with one another except for a scale factor.

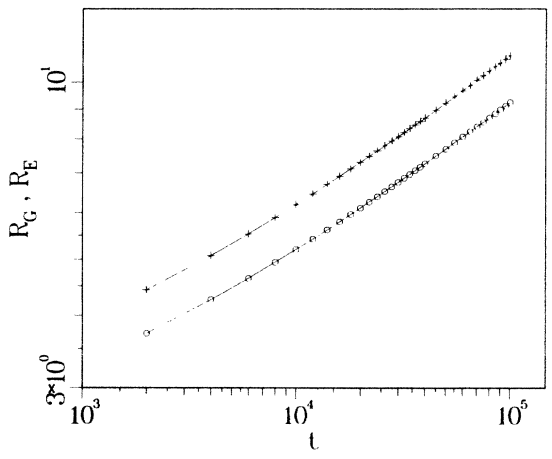

FIG. 3. Log-log plot of $R_G(t)$ and $R_E(t)$ for 32 times up to 100 000 MCS, averaged over 100 runs. R_G—pluses, R_E—circles.

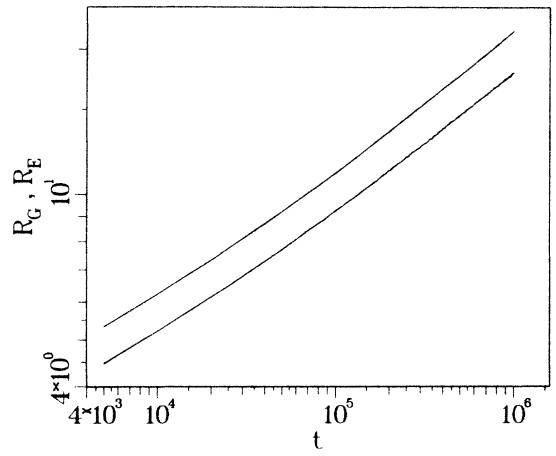

FIG. 4. Log-log plot of $R_G(t)$ and $R_E(t)$, at intervals of 5000 MCS up to 10^6 MCS, averaged over 10 runs. Upper curve is $R_G(t)$.

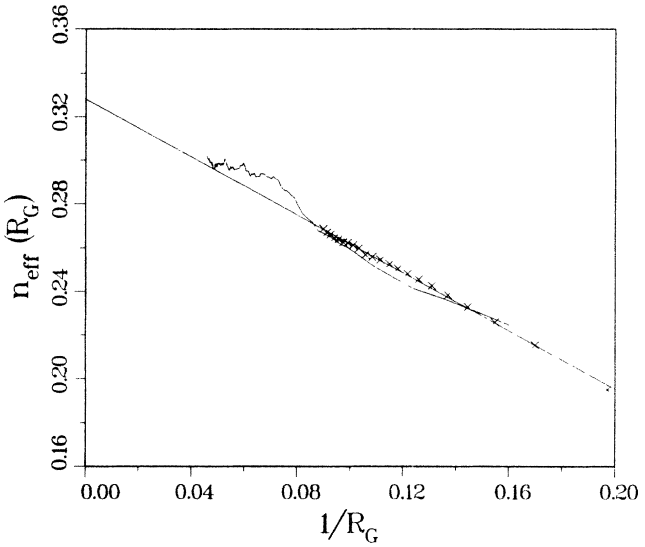

FIG. 5. Plot of effective exponent $n_{eff}(R_G)$ vs $1/R_G$. Crosses correspond to averages over 100 runs (100 000 MCS) while solid curve corresponds to 10 runs of 10^6 MCS. Straight line shown is least-squares fit to the 100-run data, with a y intercept of 0.328 ± 0.0008 and a slope of -0.665 ± 0.007.

2. *Effective exponent*

As a practical matter we have also calculated the effective exponent from our data points as

$$n_{\text{eff}}(t_f)=\ln[R(t_f)/R(t_i)]/\ln(t_f/t_i)\ , \tag{14}$$

where t_f/t_i was selected to be close to 2. In particular, for the 10^6-MCS runs t_f was taken to be all multiples of 10 000 MCS (with $t_i=t_f/2$)—resulting in 100 points. For the 10^5-MCS runs 22 values of t_f ($t_f=4000,8000,\ldots,40\,000,45\,000,\ldots,100\,000$) and for t_i, the closest values to $t_f/2$ were selected. Two was selected because it is big enough to avoid fluctuations, but small enough to observe "local time." Figures 5 and 6 show the results of effective exponents using both $R_E(t)$ and $R_G(t)$ in terms of plots of the effective exponent as a function of inverse domain size $1/R$. We note that the 10^5-MCS data (100 runs) appear to fit quite well to a straight line. The 10^6 MCS data appear to be consistent with this straight line, although the fluctuations are fairly large due to the limited number (10) of long-time runs. (This linear behavior was implicit in the early time Huse data at $T=0.9T_c$ but not clearly shown at later times.) What is more remarkable is that the y intercept or extrapolated late-time exponent appears to be very close to $\frac{1}{3}$ (see figure caption).

B. Structure factor data

1. *2D structure factor and circularly-averaged structure factor*

Figure 7 shows the increase in the peak height and the decrease of the peak position of the circularly-averaged structure factor with increasing time. We note that the structure factors for the later times are indeed much noisier due to the smaller number of runs. As a test of our simulation, and also in order to better understand the effects of the square lattice on anisotropy, we have also plotted in "gray scale" the two-dimensional structure factor for three different times (Fig. 8). We note the presence of a fourfold symmetry, indicative of the underlying lattice, which persists even into the later stages of the simulation.

2. *Scaling of circularly-averaged structure factor*

As has been shown previously in a number of studies (see, for example, Ref. 4) the circularly-averaged structure factor is expected to scale as

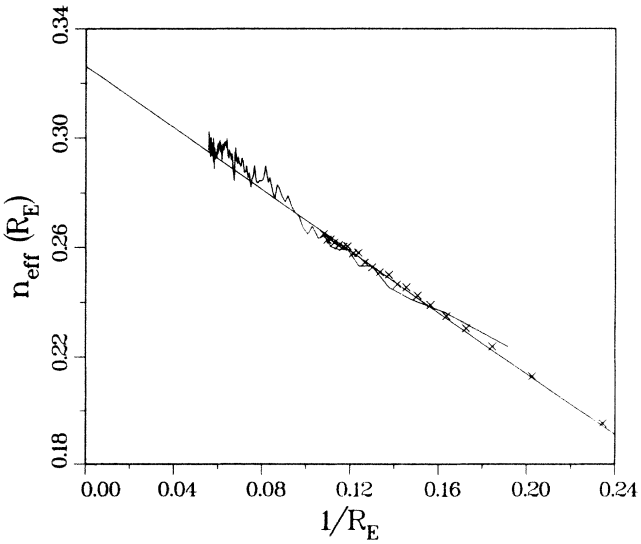

FIG. 6. Same as Fig. 5, except for R_E. Least-squares fit has a y intercept of 0.326 ± 0.003 and a slope of -0.563 ± 0.026.

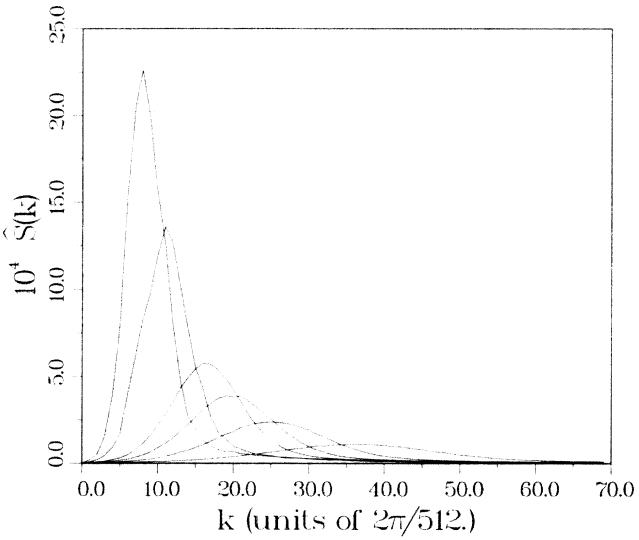

FIG. 7. Circularly-averaged structure factor $\hat{S}(k,t)$ as a function of k for six different values of t. In order of increasing peak height they are 4000 MCS, 2×10^4 MCS, 5×10^4 MCS, 10^5 MCS, 4×10^5 MCS, 10^6 MCS. Last two curves are from averages over 10 runs only.

$$\hat{S}(k,t)=Mk_1(t)^{-d}F[k/k_1(t)]\ , \tag{15}$$

where $F(x)$ is a fixed scaling function independent of time and k_1 is the first moment of the circularly-averaged structure factor (or can be any other measure of the domain size) and M is an arbitrary normalization constant. [The scaling function $F(x)$ has been found to depend weakly on temperature and minority concentration in a study by Lebowitz *et al.*[4] of growth in the three-dimensional kinetic Ising model.] In order to test if scaling holds in our simulation we have plotted

$$F(x)=(2\pi/L^2)k_1(t)^2\hat{S}(xk_1(t),t) \tag{16}$$

as a function of x for different values of t in Fig. 9. Here, the normalization constant M has been chosen such that one has

$$\int_0^\infty F(x)x\,dx=1 \tag{17}$$

in the limit that L goes to infinity, in accordance with the sum rule of Eq. (11). We note that, except for the data near the peak, the data all seem to lie on the same curve. Thus scaling appears to hold quite well. However (although this is not clearly shown in the figure), the peak height of $F(x,t)$ for times up to about 36 000 MCS is somewhat *below* the data for later times—thus causing the spread in the data near the peak shown in the figure. In addition, there is a slight increase in the peak height for later times as well. Thus, while scaling appears to hold roughly after about 36 000 MCS, there are slight deviations from scaling of the peak height even up to 100 000 MCS. The data beyond 100 000 MCS do *not* appear to show a definite increase in peak height (although the width seems to decrease slightly at low x).

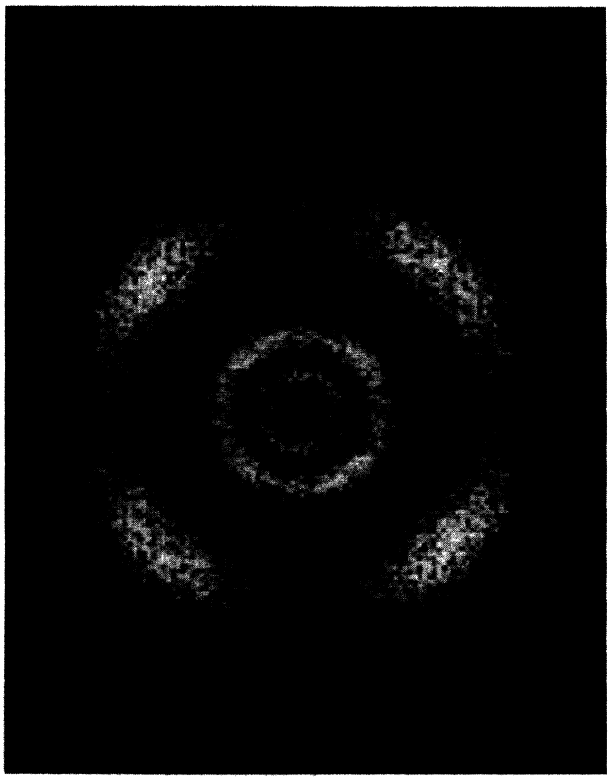

FIG. 8. Gray-scale plot (256 different levels) showing two-dimensional structure factor at three different times. In order of decreasing ring size—2000 MCS, 10^5 MCS, 10^6 MCS. Note fourfold symmetry, even at later times. Also, note the narrowing of the rings, with increasing time.

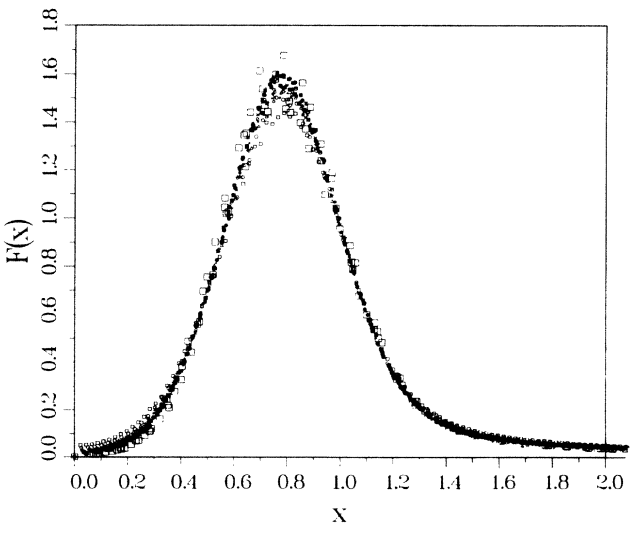

FIG. 9. Scaling function $F(x)$ superimposing data for 20 different times. Small symbols—multiples of 4000 MCS up to 40 000 MCS and from 50 000 MCS up to 100 000 MCS in steps of 10 000 MCS. Large open squares correspond to averages over 10 runs and times in multiples of 200 000 MCS up to 10^6 MCS.

However, the noisiness of these data makes it difficult to draw a definite conclusion. We note that the peak of the scaling function $F(x)$ is located at $x \approx 0.8$ instead of $x = 1$, indicating a significant contribution to the first moment k_1 beyond the peak of the circularly-averaged structure factor.

3. *Domain size obtained from moments*

Figures 10 and 11 show log-log plots of the domain size $R_1(t)$ and $R_2(t)$ as obtained from the circularly-averaged structure factor. We note that the curves for $R_1(t)$ and $R_2(t)$ are not quite parallel, indicating that the two measures of domain size are not equivalent. The effective exponents for these two measures of domain size, calculated as discussed above, are shown in Figs. 12 and 13. We note that the effective exponent calculated from the first moment (R_1) is comparable to that calculated from the energy and pair-correlation function, again fitting a straight line with y intercept very close to $\frac{1}{3}$. The results for the second moment, however, yield a y intercept somewhat below that from R_1. This, however, is not surprising, given the greater sensitivity of the second moment to noise in the data and the choice of cutoff.

C. Fits to $T = 0.5T_c$ data

Thus, our data for the effective exponents for $R_E(t)$, $R_G(t)$, and $R_1(t)$ (when extrapolated linearly as a function of $1/R$) seem to point fairly clearly to a long-time growth exponent very close to $\frac{1}{3}$. Table I shows a summary of values obtained from linear least-squares fits to our plots of $n_{\text{eff}}(R)$ versus $1/R$. Included are the results of least-squares fits to the long-time data. We note that, even though these results are not expected to be as accurate (due to the smaller number of runs), they give extrapolated values of the long-time growth exponent which are not too different from those obtained from the shorter-run data. Averaging the extrapolated values for the long-time exponent from the 100-run data for $R_E(t)$, $R_G(t)$, and $R_1(t)$ yields a value for the long-time growth exponent of 0.330 ± 0.005.

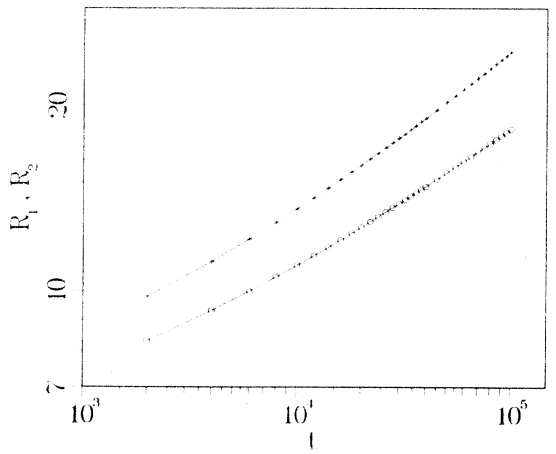

FIG. 10. Log-log plot of $R_1(t)$ (pluses) and $R_2(t)$ (circles) averaged over 100 runs.

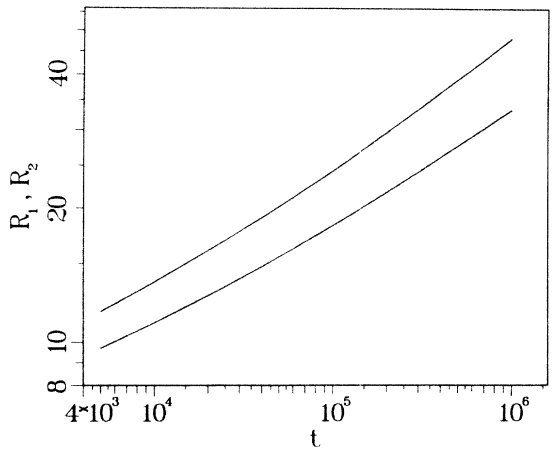

FIG. 11. Log-log plot of $R_1(t)$ (upper curve) and $R_2(t)$ in steps of 5000 MCS up to 10^6 MCS.

Surprisingly, the linear behavior of $n_{\text{eff}}(t)$ as a function of $1/R$ seems to hold even for fairly early times. As previously noted, this is equivalent to the form

$$R(t) = A + Bt^{1/3}, \tag{18}$$

where $A = 3C$. In order to test the conjecture that this is in fact a good expression for the growth of domain size as a function of time, for all but early times, we have performed least-squares fits to our data using Eq. (18). Figure 14 shows the data for $R_E(t)$ and $R_G(t)$ from the 10 runs of 10^6 MCS superimposed with the fit to

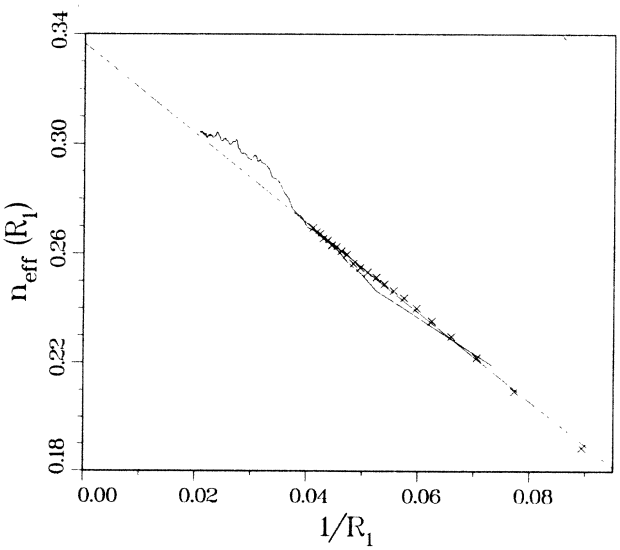

FIG. 12. Effective exponent $n_{\text{eff}}(R_1)$ vs $1/R_1$. The $\times$'s correspond to data over 100 runs up to 10^5 MCS, solid curve to 10^6-MCS data (10 runs). Least-squares fit to 100-run data has a y intercept of 0.336 ± 0.0007 and a slope of -1.633 ± 0.014.

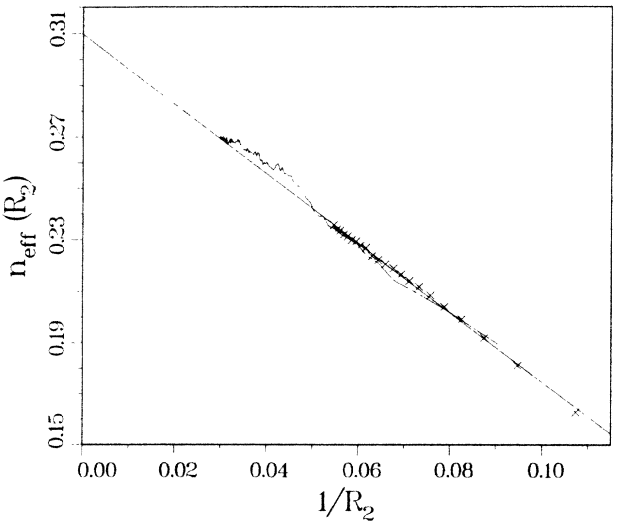

FIG. 13. Same as Fig. 10 but for R_2. Least-squares fit has a y intercept of 0.310 ± 0.0008, slope of -1.353 ± 0.013.

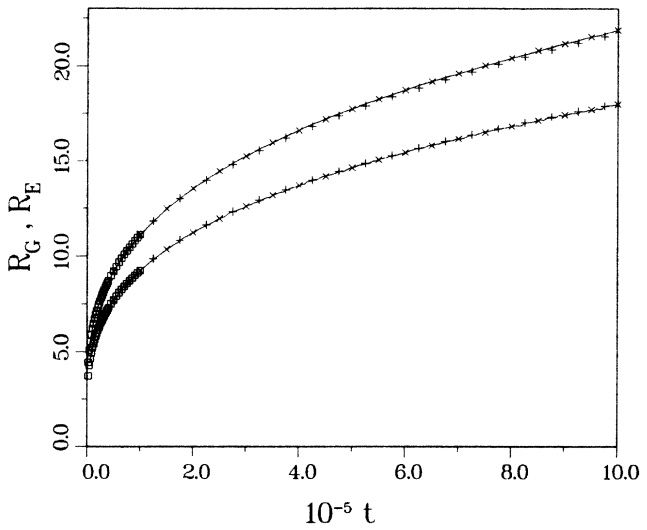

FIG. 14. Linear plot of domain size vs time for R_G and R_E with accompanying fits: solid lines—10^6-MCS data, open squares—10^5-MCS data, crosses—fits of form of Eq. (18) to 10^6 MCS data, pluses—fits of form of Eq. (18) to 10^5-MCS data (extrapolated). Coefficients of fits for 10^6-MCS data are for R_G, $A=1.829$ and $B=0.2003$; for R_E, $A=1.694$ and $B=0.1629$.

these data using Eq. (18). We see that the fits are excellent. In addition, the fits to the early-time data (100 000 MCS, 100 runs) extrapolated to 10^6 MCS are also shown. We note that there is excellent agreement in the case of $R_E(t)$, while in the case of $R_G(t)$ the deviation of the later-time (10^6 MCS) data from the extrapolated fit is about one and a half times the estimated error $\delta R_G(t)$ from fluctuations. Figure 15 shows an expanded view of the early-time data along with the fit (again error bars are not shown since they are too small). As a measure of the accuracy of the early-time data, we have plotted in Fig. 16 the estimated relative error (calculated from fluctuations over 100 runs) in $R_G(t)$ and $R_E(t)$ as a function of time. In Fig. 17, we have plotted the relative error of the fit to the early-time data using Eq. (18) to fit the data. The average relative error of the fit [about 0.05% for $R_G(t)$ and about 0.1% for $R_E(t)$] is of the order of the average estimated relative statistical error [about 0.07% for both $R_G(t)$ and $R_E(t)$]. Figure 18 shows the relative error of the fit to the longer-time (10^6 MCS, 10 runs) data. The average relative error of the fit to this data is about twice that for the shorter-time data but is less than (0.15% versus 0.4%) the estimated relative error from fluctuations.

TABLE I. Extrapolated long-time exponents at $T=0.5T_c$ using least-squares fits of the form $n_{eff}(1/R)=D-C/R$ to data.

	100 runs	10 runs
$n_{eff}(R_E)$	0.326±0.003	0.337±0.001
$n_{eff}(R_G)$	0.328±0.0008	0.336±0.001
$n_{eff}(R_1)$	0.336±0.0007	0.344±0.0009
$n_{eff}(R_2)$	0.310±0.0008	0.315±0.0008

Figures 19 and 20 show fits, similar to those in Figs. 14 and 15, but for the domain size R_1 obtained from the first moment of the circularly-averaged structure function $\hat{S}(k,t)$. We note that the extrapolated short-time fit for $R_1(t)$ in Fig. 19 does not agree quite as well with the long-time data as the data in Fig. 14. However, as previously mentioned there is a moderate amount of uncertainty in R_1, due not only to the small number of runs

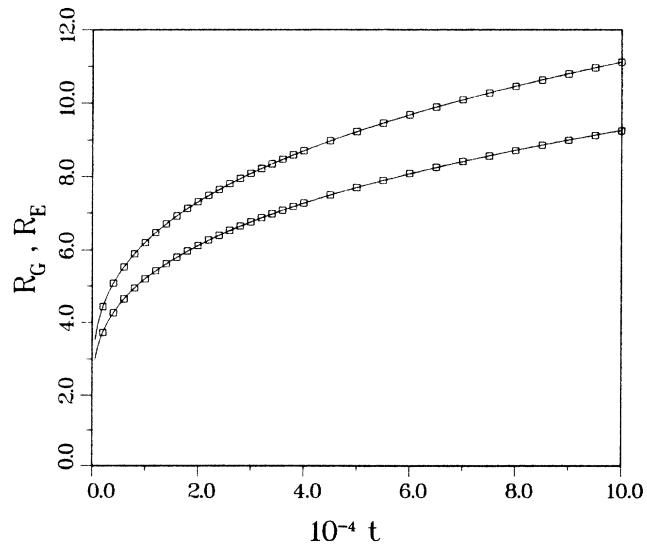

FIG. 15. Expanded linear plot of $R_G(t)$ and $R_E(t)$ for 10^5-MCS data with accompanying fits (solid lines). Coefficients of fits are for R_G, $A=1.942$ and $B=0.1977$; for R_E, $A=1.679$ and $B=0.1634$.

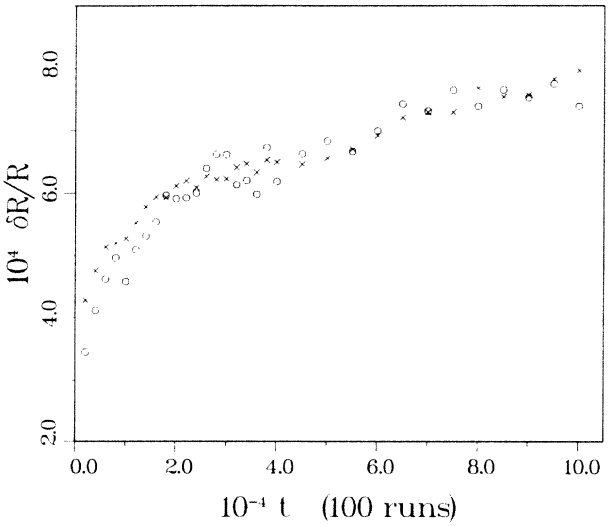

FIG. 16. Estimated relative statistical error $\delta R/R$ in R_G (crosses) and R_E (open circles) for data over 100 runs.

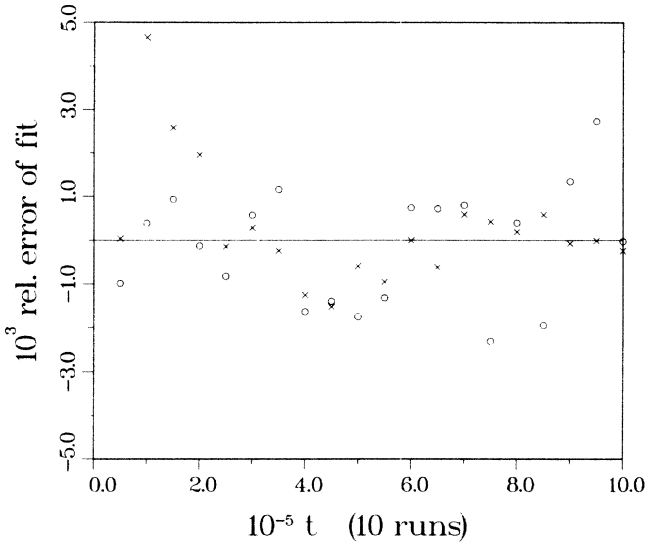

FIG. 18. Relative error of fits to 10^6-MCS data for times at intervals of 50 000 MCS. Crosses—R_G, open circles—R_E.

(10) but also to the dependence on the cutoff. Thus, it is not clear whether the observed deviations of the extrapolated short-time data from the longer-time data are due to these uncertainties or are in fact indications of a next-order correction to the form of Eq. (1). Table II shows a summary of our fits to the data at $T=0.5T_c$ for all three measures of domain size.

As an aside, it is interesting to note that for the 100-run data, the relative statistical error $\delta R/R$ for all three measures of domain size—R_E (see Fig. 16), R_G (see Fig. 16), and R_1 (not shown)—is approximately the same at a given time. Since we already know (see Ref. 7) that the energy per spin $E(t)$ is a self-averaging quantity [whose relative error decreases with system size as $\delta E/E \sim (1/N^{1/2})$, where N is the number of spins in the system], then this suggests that the other two measures of domain size—R_G and R_1—are also self-averaging. In the case of R_1 this is not too surprising if one considers that the dominant part of the circularly-averaged structure function $\hat{S}(k,t)$ involves an average over the structure factor of order $N^{1/2}$ points while the first and

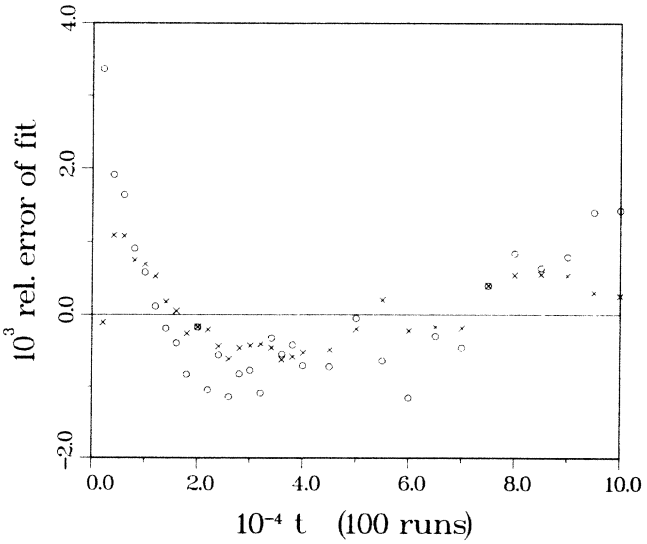

FIG. 17. Relative error of fits to 10^5-MCS data. Symbols same as in Fig. 16.

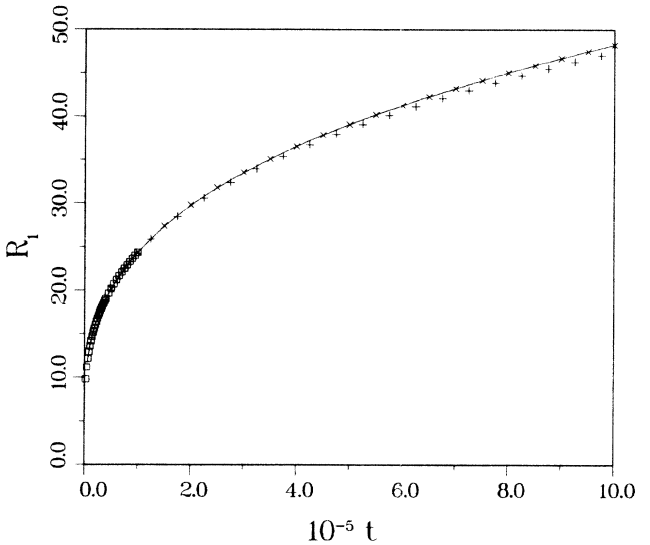

FIG. 19. Plot of $R_1(t)$ with fit out to 10^6 MCS. Solid curve—data from 10 runs. Large open squares—data from 100 runs of 10^5 MCS. Crosses—fit to 10^6-MCS data. Pluses—fit to 10^5-MCS data extrapolated to 10^6 MCS. Coefficients of fit to long-time data are $A=3.699$ and $B=0.4314$.

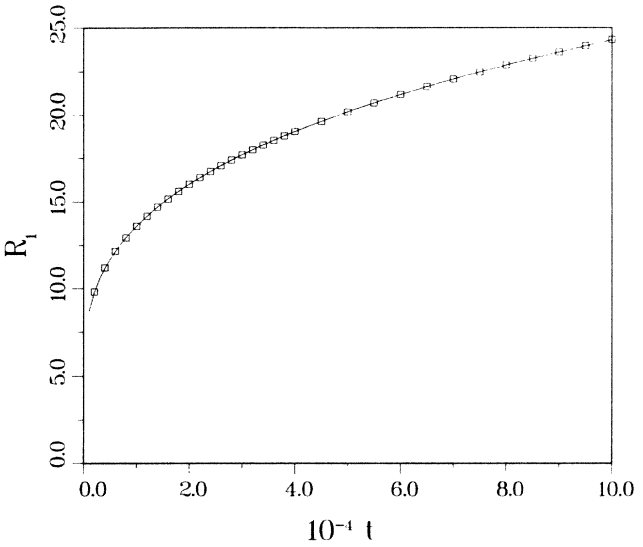

FIG. 20. Expanded plot of 10^5-MCS data (open squares) with fit (solid curve) for $R_1(t)$. Coefficients of fit are $A=4.331$ and $B=0.4307$.

second moments involve a further average up to a cutoff of order $L=N^{1/2}$ points. Similarly, the pair-correlation function involves, like the energy, an average over (N/ξ^2) independent samples. We note that since $R_E(t)$ is given by Eq. (8), and assuming that one has, as in equilibrium,

$$\Delta E(t)=(k_B T^2 C_H)^{1/2}/N^{1/2} ,$$

this implies that the relative variance

$$\Delta R_E/R_E=\tfrac{1}{2}(k_B T^2 C_H)^{1/2} R_E/N^{1/2} .$$

Thus, the relative error in R_E should increase with increasing domain size as is observed (see Fig. 16). We note, however, that the constant of proportionality is somewhat larger than predicted above. Inserting the appropriate values in the above formula at $T=0.5T_c$ for $t=10^5$ MCS [and dividing by $(N_r-1)^{1/2}$ to get the relative error] gives a predicted value for

$$(\delta R_E/R_E)_{\text{pred}}=2.2\times 10^{-4}$$

while the observed value of $\delta R_E/R_E$ at 10^5 MCS is (see Fig. 16) about 7×10^{-4}. A more careful study of the variation of δR_E with time will, however, require much better statistics.

D. Data for $T=0.3T_c$

As a comparison with the results at $T=0.5T_c$ we have also conducted one run of 10^6 MCS at $T=0.3T_c$. Figure 21 shows a plot of the effective exponent $n_{\text{eff}}(R_G)$ as a function of inverse domain size. A plot of $n_{\text{eff}}(R_E)$ versus $1/R_E$ shows a similar behavior, with a least-squares fit whose y intercept gives a value for the effective exponent at long times somewhat below the value for $R_G(t)$. We see that, due to the low temperature, the fluctuations are relatively small. Figure 22 shows the behavior of $R_G(t)$ and $R_E(t)$ as a function of t along with fits of the form of Eq. (18). Again we see an excellent fit to the data over a range of 10^6 MCS. While these results may not be considered to be statistically significant, they clearly agree with those presented earlier.

IV. DISCUSSION

The results presented so far indicate that, even at low temperatures, and with a "critical" concentration, the long-time growth exponent is in fact $\frac{1}{3}$. What is more striking is that the data can all be quite accurately fit (within the accuracy of our simulation) by the simple form given by Eq. (18): $R(t)=A+Bt^{1/3}$. Thus, it would appear that an excellent fit is provided by Eq. (18), and that in the future, the problem will center more on the determination of the value of the coefficients A and B as functions of temperature and concentration. Table II shows the values for A and B for R_E, R_G, and R_1 for both the short-time and the long-time data and the relative differences between them. We note that the relative error in A tends to be somewhat larger than for B.

One point which should be stressed is that, as pointed out earlier in our discussion of statistical error, the quantities which we have used for the determination of domain size as a function of time are all *self-averaging*. That is, their relative statistical error decreases not only with the number of independent runs but also with the *size* of the system. This is to be contrasted with certain measures of domain size used in the study of growth with *nonconserved* order parameter (such as the mean square of the magnetization per spin) which are *not* self-averaging.[7,13] For these measures of domain size the relative statistical error is independent of system size and decreases only with the number of runs.

If we consider the results of this work at $T=0.5T_c$ and $0.3T_c$ and of previous work[4,6] at $T=0.9T_c$ and at

TABLE II. Coefficients A and B at $T=0.5T_c$ using linear least-squares fits of form of Eq. (18) to data. Last two rows show values for A obtained from slopes of $n_{\text{eff}}(R)$ vs $1/R$ for comparison

	A_E	B_E	A_G	B_G	A_1	B_1
100 runs (10^5 MCS)	1.679	0.1634	1.942	0.1977	4.331	0.4307
10 runs (10^6 MCS)	1.694	0.1629	1.829	0.2003	3.729	0.4452
% difference	0.89	−0.31	−5.8	1.3	−13.9	3.3
$3C$ (100 runs)	1.690		1.994		4.90	
$3C$ (10 runs)	1.824		2.158		5.25	

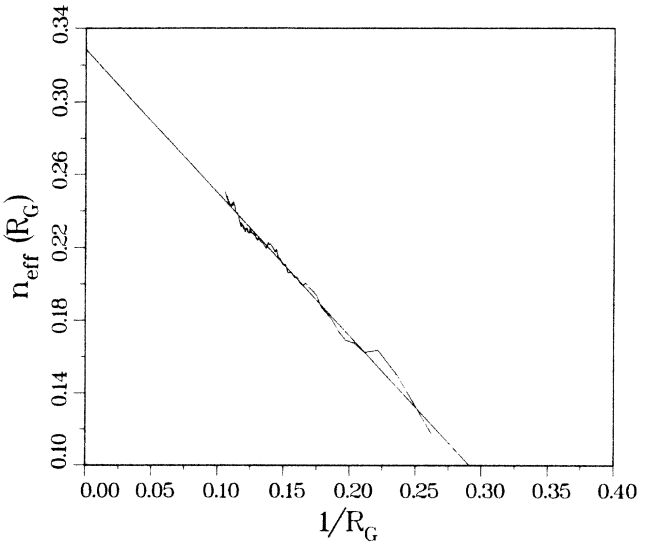

FIG. 21. Plot of $n_{\text{eff}}(R_G)$ vs $1/R_G$ at $T=0.3T_c$ from one run of 10^6 MCS. Straight line is least-squares fit with a slope of -0.7854 ± 0.009 and y intercept of 0.329 ± 0.001.

minority concentration in the light of Huse's phenomenological theory, as embodied in Eqs. (1)–(4), it is possible to get a better understanding of the growth law as a function of temperature and concentration. In what follows, we compare our results and those of other simulations[4,6] with the predictions of Huse's theory. While some of the data used in our comparison are somewhat tentative (or based on a limited number of runs or "early-time" data), we feel that they are sufficiently accurate for the type of comparison which we wish to make.

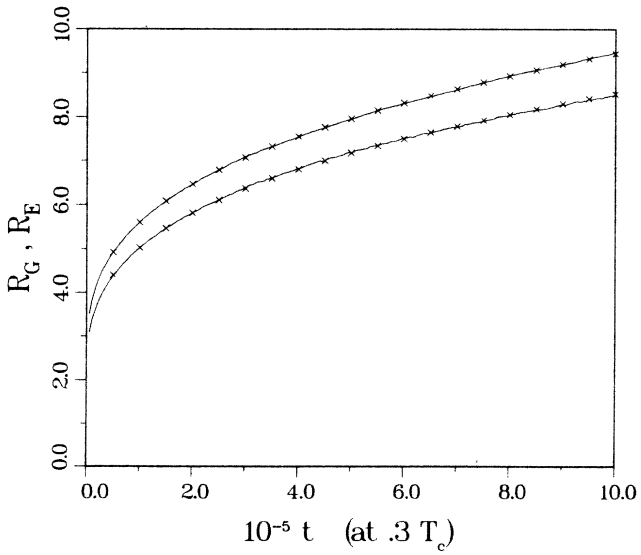

FIG. 22. Plot of $R_G(t)$ and $R_E(t)$ data at $T=0.3T_c$ from one run of 10^6 MCS (solid curves) along with fits of the form of Eq. (18) (crosses). Coefficients of fit are for R_G, $A=2.275$ and $B=0.0716$; for R_E, $A=1.995$ and $B=0.0653$.

A. Variation of effective exponent with concentration of minority phase

Lebowitz *et al.*,[4] in a simulation of spinodal decomposition for the three-dimensional Ising model at $T=0.59T_c$, measured an exponent of 0.33 for an off-critical quench (5% concentration, $T=0.59T_c$) while the value of the effective exponent n [when fit to the form $R(t)\sim t^n$] appeared to be about 0.2 for simulations with *equal* phase concentrations. The first value of the exponent is explained by the fact that for minority concentration, there will be, as pointed out by Huse, very little growth of domains due to surface conduction. Thus the correction to the $\frac{1}{3}$ growth law at early times is very small. For equal concentrations the surface conduction becomes important at early times so that one sees a slowly increasing exponent near 0.2 if one does a simple fit of form $R(t)\sim t^n$.

B. Variation with temperature of slope of $n_{\text{eff}}(R)$ versus $1/R$ at critical concentration

Huse has suggested (see Ref. 6) that at low temperature, the surface-conduction coefficient C_3 should decrease less rapidly than the bulk-conduction coefficient C_2, since surface conduction may involve processes which require less energy than bulk conduction.[16] This implies that with decreasing temperature, the slope $C=C_3/6C_2$ (and $A=3C$) should increase. While this is *qualitatively* consistent with the results of our simulations and those of Huse at $0.9T_c$, the observed increase in the slope C with decreasing temperature is much *less* than the exponential factor $C\sim\exp(4J/T)$ suggested by Huse's arguments. Using the results obtained from our simulations, we obtain[17]

$$C_G(0.3T_c)/C_G(0.5T_c)\simeq 1.18\ ,$$

while $\exp(4\Delta J/T)\simeq 5.33$. Thus, it is plausible[18] that, rather than increasing exponentially with decreasing temperature, the slope C approaches a finite value in the limit of zero temperature. This is also consistent with the observed freezing[2] at a *finite* value of $R(t)$ at $T=0$.

C. Variation of long-time growth coefficient B with temperature at critical concentration

Using arguments similar to those used by Lifshitz[19] in a study of nonconserved order-parameter growth, Huse obtained as a formula for the long-time growth coefficient B [see Eq. (5) of Ref. 6],

$$B=(3C_2)^{1/2}\sim(\lambda\Sigma/M^2)^{1/3}\sim(D\chi\Sigma/M^2)^{1/3}\ , \qquad (19)$$

where $\lambda=D\chi$ is the bulk spin conductivity, D is the diffusion coefficient, χ is the magnetic susceptibility, Σ is the surface free energy, and M is the magnetization per spin. Assuming that the coefficient of diffusion D is independent of temperature at low temperature, and using values of χ obtained from low-temperature series expansions,[20] using for M the exact Onsager expression,[21] and using for Σ the average of the exact expressions for the surface free energy of the Ising model in the principal[14] and diagonal[22] directions, we obtain

$$[B(0.5T_c)/B(0.3T_c)]_{\text{pred}}=2.7 .$$

Using our simulation values we obtain

$$B_E(0.5T_c)/B_E(0.3T_c)=2.5$$

and

$$B_G(0.5T_c)/B_G(0.3T_c)=2.75 ,$$

which is not too different from the predicted value. Thus, while this agreement may be fortuitous, it is tempting to believe that Eq. (19) does in fact express quantitatively correctly the variation of $B(T)$ with temperature at low temperatures.

However, Eq. (19) does not appear to describe the temperature variation of $B(T)$ at higher temperatures. Thus, if we calculate the value of

$$B_G(0.9T_c)/B_G(0.5T_c)$$

obtained from our simulations [using Huse's early-time data we obtained a value of $B_G(0.9T_c)\approx 0.40$, in rough agreement with a run we did ourselves] we get

$$B_G(0.9T_c)/B_G(0.5T_c)\approx 2.0 .$$

Using Eq. (19) and substituting values for the spin conductivity λ which we obtained from additional Monte Carlo simulations,[23,24] we obtain

$$[B_G(0.9T_c)/B_G(0.5T_c)]_{\text{pred}}\simeq 1.5 ,$$

lower than our simulation value by about 25%. We note, however, that our estimate for $B_G(0.9T_c)$ from simulations is based on early-time data and may not be too accurate. Thus it is not clear whether the discrepancy between the predicted and measured values of B_G at $T=0.9T_c$ is due to some factor not taken into account in Eq. (20) at high temperatures (such as a variation in the "geometry" of the domains with temperature) or is simply due to an inaccurate value of $B_G(0.9T_c)$. We note in this connection that at high temperatures one expects fluctuations to be very large and thus a larger number of runs may be required to determine the correct long-time behavior. At the same time the domains grow relatively fast, further increasing the error. A more detailed discussion of the temperature and concentration dependence of the coefficients A and B will have to await further simulations.

ACKNOWLEDGMENTS

We would like to acknowledge the assistance of Dr. Roy Wessel of Control Data Corporation (CDC) for invaluable early contributions to the programming, Dr. Hai C. Tang of the Computer Services Division of the National Bureau of Standards for help with the laser graphics in Fig. 2 and with the fast Fourier transform, and Richard Freemire for the production of the gray-scale plot shown in Fig. 8. In addition, we would like to acknowledge valuable conversations with Professor Theodore L. Einstein and Dr. Jeffrey Marqusee. One of us (J.G.A.) was supported in part by the National Research Council.

[1] I. M. Lifshitz and V. V. Slyozov, J. Phys. Chem. Solids **19**, 35 (1961).

[2] G. F. Mazenko, O. T. Valls, and F. C. Zhang, Phys. Rev. B **31**, 4453 (1985); **32**, 5807 (1985).

[3] M. Rao, M. H. Kalos, J. L. Lebowitz, and J. Marro, Phys. Rev. B **13**, 4328 (1976).

[4] J. L. Lebowitz, J. Marro, and M. H. Kalos, Acta Metall. **30**, 297 (1982).

[5] G. S. Grest and D. J. Srolovitz, Phys. Rev. B **30**, 5150 (1984).

[6] D. A. Huse, Phys. Rev. B **34**, 7845 (1986).

[7] A. Milchev, K. Binder, and D. W. Heermann, Z. Phys. B **63**, 521 (1986).

[8] N. Metropolis, A. W. Rosenbluth, M. N. Rosenbluth, A. H. Teller, and E. Teller, J. Chem. Phys. **21**, 1087 (1954). [The probability for an exchange is given by $\exp(-\Delta E/kT)$ if the exchange costs energy $\Delta E>0$, and by 1 if $\Delta E\leq 0$.] This is the same algorithm as used in Ref. 6. We note that this algorithm is different from the usual "tanh" algorithm used in dynamics studies, in which the pair-exchange probability is given by $\frac{1}{2}[1-\tanh(\Delta E/2kT)]$. However, we do not expect the long-time behavior or universality class to be affected by this difference in the microscopic dynamics. In this connection, we note that at the fairly low temperatures of our simulation the only difference—to first order—between the Metropolis algorithm and the "tanh" algorithm is for those exchanges corresponding to diffusion ($\Delta E=0$), for which the Metropolis algorithm gives probability 1, while the "tanh" algorithm gives probability $\frac{1}{2}$.

[9] F. Sullivan and R. D. Mountain, in *Proceedings of the First Symposium on the Frontiers of Massively Parallel Scientific Computing*, edited by J. R. Fischer, NASA Goddard Space Flight Center, Greenbelt, Maryland, NASA Conf. Publ. No. 2478 (U.S. GPO, Washington, D.C., 1986).

[10] See, for example, S. Wansleben, J. G. Zabolitsky, and Claus Kalle, J. Stat. Phys. **37**, 271 (1984).

[11] G. Bhanot, D. Duke, and R. Salvador, J. Stat. Phys. **44**, 985 (1986).

[12] We note that, in our simulation, the generation of a pool of $(128)^3$ pairs of random "demon" bits [which were updated or "refreshed" every 20 MCS and from which a subset of size $(128)^2$ was randomly selected before each vectorized exchange] took about half the simulation time. Lowering the refresh frequency (to say, once every 100 MCS) could have increased the speed of the simulation by about 50%. However, to avoid possible problems due to spurious correlations we updated more frequently.

[13] E. T. Gawlinski, Martin Grant, J. D. Gunton, and K. Kaski, Phys. Rev. B **31**, 281 (1985).

[14] L. Onsager, Phys. Rev. **65**, 117 (1944).

[15] A. Sadiq and K. Binder, J. Stat. Phys. **35**, 517 (1984).

[16] In the limit of very low temperature, one has [see Eq. (19)]

$$C_2\sim\chi\sim(1-M)/T\sim(J/T)\exp(-8J/T) .$$

According to Huse's arguments, the surface conductivity λ_s should vary as $\exp(-4J/T)$ at low temperature, and thus if $C_3 \sim \lambda_s$ then one has, including only exponential factors

$$C = C_3/6C_2 \sim \exp(4J/T) .$$

[17]If we use Eq. (19) to evalute C_2 [and again assuming that $C_3(T) \sim \exp(4J/T)$] we obtain

$$C(0.3T_c)/C(0.5T_c) \simeq 3.56$$

which is still much larger than 1.18. Thus, the dependence of the coefficient C_3 on the surface conductivity may not be quite so simple as suggested by Huse.

[18]A consideration of the energetics of the migration of an overturned spin at an interface near an interface step indicates that for steps of height one there is an energy cost of $8J$ while for steps greater than one the energy cost is $4J$. In the limit of low temperature and late time, we expect steps of height one to dominate. Thus, it may not be too surprising that the surface-conduction coefficient C_3 decays as rapidly as the bulk-conduction coefficient C_2.

[19]I. M. Lifshitz, Zh. Eksp. Teor. Fiz. **42**, 1354 (1962) [Sov. Phys.—JETP **15**, 939 (1962)].

[20]M. F. Sykes, D. S. Gaunt, J. L. Martin, S. R. Mattingly, and J. W. Essam, J. Math. Phys. **14**, 1073 (1973).

[21]L. Onsager, Nuovo Cimento **6**, 249 (1949).

[22]M. E. Fisher and A. E. Ferdinand, Phys. Rev. Lett. **19**, 169 (1967). See also C. Rottman and M. Wortis, Phys. Rev. B **24**, 6274 (1981).

[23]We have measured the bulk spin conductivity λ directly at $T = 0.9T_c$ and $0.5T_c$ by applying a small field (in a one-phase sample) favoring exchanges in one direction and measuring the resulting spin current density (see, for example, Ref. 24). Using a system of size 55×55 at $T = 0.5T_c$ and 60×60 at $T = 0.9T_c$, we find

$$[\lambda(0.9T_c)/\lambda(0.5T_c)] \simeq 12.2 .$$

[24]S. Katz, J. L. Lebowitz, and H. Spohn, J. Stat. Phys. **34**, 497 (1984).

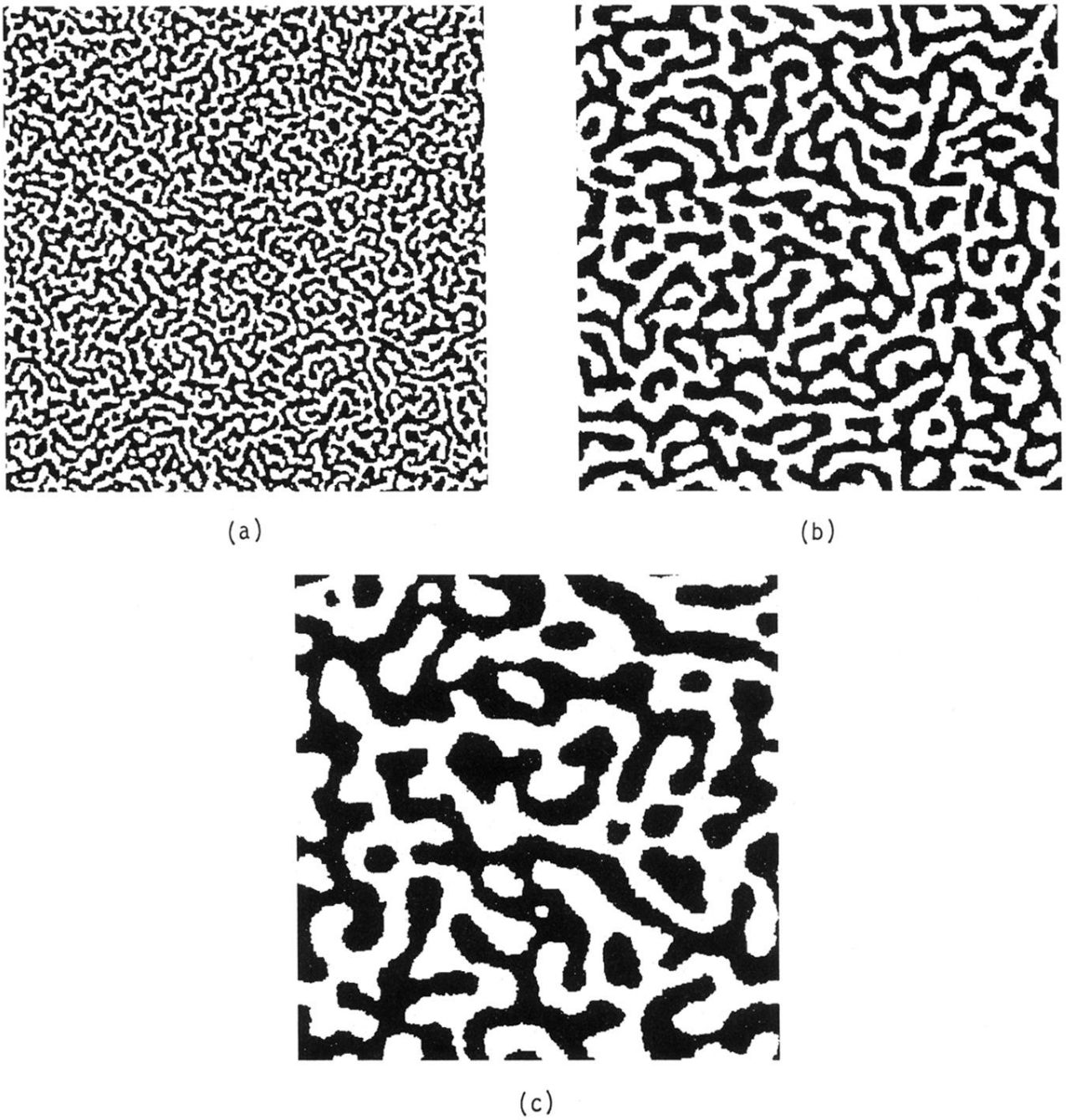

FIG. 2. View of 512×512 lattice in the course of one run (at $T = 0.5 T_c$) at three different times: (a) 5000 MCS, (b) 100 000 MCS, and (c) 980 000 MCS.

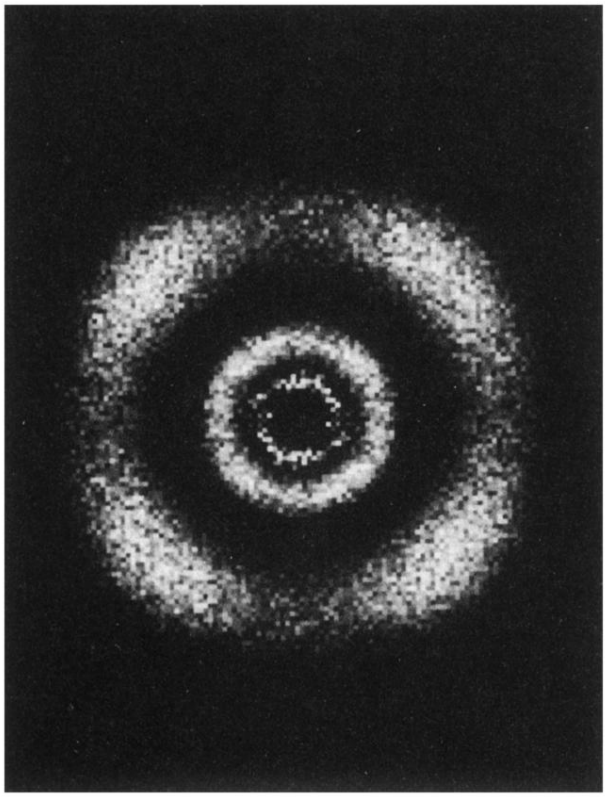

FIG. 8. Gray-scale plot (256 different levels) showing two-dimensional structure factor at three different times. In order of decreasing ring size—2000 MCS, 10^5 MCS, 10^6 MCS. Note fourfold symmetry, even at later times. Also, note the narrowing of the rings, with increasing time.